# Isotopic labeling studies of interactions of nitric oxide and nitrous oxide with ultrathin oxynitride layers on silicon

H. C. Lu,[a] E. P. Gusev,[b] E. Garfunkel, B. W. Busch, and T. Gustafsson
*Departments of Physics and Chemistry, Rutgers University, Piscataway, New Jersey 08854-8019*

T. W. Sorsch and M. L. Green
*Bell Laboratories, Lucent Technology, Murray Hill, New Jersey 07974*

The interaction of nitric (NO) and nitrous ($N_2O$) oxide with ultrathin ($\sim 1.5$–3.5 nm) oxide and oxynitride films on silicon has been studied by performing high resolution depth profiling using medium energy ion scattering and isotopic labeling methods. We observe that, after NO annealing at 850 °C, both O and N incorporate near the $SiO_2$/Si interface. There is no nitrogen and little newly incorporated oxygen observed at the surface, implying that NO diffuses through the oxide film and dissociates and reacts at the interface. For $N_2O$ annealing, atomic oxygen resulting from decomposition of the gas can replace oxygen atoms in both oxide and oxynitride films. This replacement is most important at the surface, but also, to a smaller extent, occurs in the middle of the film. For ultrathin oxynitride films, oxide growth during reoxidation is faster in $N_2O$ than in pure $O_2$. Atomic oxygen also influences the nitrogen distribution, which moves further into the film and accumulate at the new interface. We discuss the roles of atomic oxygen and peroxyl bridging oxygen species in explaining the observed phenomena. © *2000 American Institute of Physics.* [S0021-8979(00)01303-7]

## I. INTRODUCTION

Silicon oxynitride films grown thermally using NO (nitric oxide) and $N_2O$ (nitrous oxide) exhibit electrical properties that under the correct conditions are superior to pure oxide films, including suppressed dopant (boron) penetration and improved hot-electron immunity.[1–7] These processes have great technological potential due to the relative ease of accommodating the gases in current production facilities. Although the mechanisms of silicon oxynitridation with NO and $N_2O$ are understood at the monolayer level (the ''surface science limit''),[8–14] less is known about the atomistic steps involved in the oxynitridation reactions for somewhat thicker, 1–5 nm films (the ''ultrathin film regime'').

For low exposures at room temperature, several studies show that NO molecules are chemisorbed dissociatively on both Si(100)-(2×1) and Si(111)-(7×7) surfaces.[8,11,15,16] The resulting films show an N/O ratio of $\sim 0.8$–1 with submonolayer coverages. An N/O ratio >1, or even a pure nitride layer, can be achieved through cyclic adsorption and annealing to high temperatures to selectively desorb O (in the form of SiO).[10,15,16] For much higher exposures at $\sim 800$–1000 °C, $\sim 1.5$–2.5 nm thick films can be formed. These films often show an N/O ratio of $\sim 0.1$ when grown at high pressures ($\sim 50$–100 Torr NO partial pressure).[17,18] This ratio increases with decreasing pressure[19] and increasing temperature.[17] NO can also be used to incorporate nitrogen into $SiO_2$ films on Si. In this case, the nitrogen atoms are incorporated near the $SiO_2$/Si interface.[3,7,17,20–22] A recent

isotopic labeling study using nuclear reaction analysis (NRA) by Baumvol *et al.*[23] has found two reactions for a 6.5 nm thick oxide annealed in NO at 1050 °C. A significant fraction of the oxygen atoms in $SiO_2$ near the surface was replaced by O atoms from NO, while both N and O were found to incorporate at the interface. It was not clear through which path nitrogen reaches the interface, and both N and NO diffusion through the film were considered.

At room temperature, Si(100)-(2×1) does not absorb $N_2O$ except at surface defects,[13,14] while at low temperatures molecular adsorption may occur. Upon heating, the molecule dissociates and silicon oxide is formed while molecular nitrogen desorbs.[12] The high-temperature gas-phase chemistry of nitrous oxide is known to be quite complex. At $\sim 900$ °C or higher, $N_2O$ is quite unstable and dissociates, forming atomic oxygen and molecular nitrogen. Through a series of gas-phase reactions, an equilibrium is eventually obtained which consists predominantly of $N_2$, $O_2$, and NO.[24–29] To understand $N_2O$ oxynitridation in a low flow-rate furnace (where relatively long delays occur between gas heating and the reaction at the silicon wafer), one needs to consider the reaction(s) between the $SiO_xN_y$/Si system and the more stable decomposition products, $N_2$, $O_2$, and NO.[24,30] On the other hand, $N_2O$ oxynitridation in a high flow-rate furnace or RTO (where the heat is applied directly to the wafer) allows more of both the $N_2O$ and the intermediate (metastable) gas-phase species, such as atomic oxygen, to reach the wafer. These considerations have a direct bearing on understanding the differences between properties of films produced with different procedures.

A basic question that arises when trying to understand the oxynitridation mechanism is how O and N move in the

[a]Electronic mail: hclu@physics.rutgers.edu
[b]Present address: IBM Thomas J. Watson Research Center, P.O. Box 218, Yorktown Heights, NY 10598.

films. It is possible to trace atomic movements using various isotopic labeling methods. Ganem *et al.* have used NRA to study silicon oxynitridation in $N_2O$ for somewhat thicker films ($\gtrsim 10$ nm).[31,32] In studies of ultrathin films ($\sim 1.5$–3.5 nm films are of interest in our work), high resolution is preferred. We have used medium energy ion scattering (MEIS), which has a depth resolution of $\sim 0.5$ nm under favorable conditions, and which we have applied earlier to high-resolution depth profiling studies of silicon oxides[33,34] and oxynitrides.[17,21,35,36]

## II. EXPERIMENT

$Si^{18}O_2$ and $Si^{16}O_2$ samples were grown at 1000 °C on Si(100) in a rapid thermal processing (RTP) reactor. These samples then went through various treatments in NO and $N_2O$ before ion scattering was performed for depth profiling. The NO ($N^{16}O$) annealing ($\sim 100$ Torr partial pressure diluted by $N_2$, 850 °C) was performed in a vertical furnace. For $N_2O$ annealing ($N_2^{16}O$, 1.5–14 Torr, 900–1000 °C), small rectangular samples were cut from 6 in. wafers and loaded in a closed quartz furnace, consisting of a 1 in. quartz tube attached to an ultrahigh vacuum (UHV) chamber (base pressure $<1\times10^{-9}$ Torr) equipped with a residual gas analyzer (RGA). The heated part accounts only for a small portion of the whole volume of the furnace and it takes 10–30 min for $N_2O$ to fully decompose in the temperature range used. Since the typical annealing time is one hour, the sample is effectively annealed in oxygen for the later part of this time. The effect of $N_2O$ is deduced from a comparison with annealing in pure oxygen gas for one hour.

The MEIS setup has been described elsewhere.[37,38] We use $\sim 100$ keV protons. This energy is near the energy loss maximum of protons in $SiO_2$, which, when combined with a high resolution electrostatic energy analyzer, results in high depth resolution ($\sim 0.5$ nm for ultrathin films). The energy spectra of the backscattered protons can be analyzed to obtain information about the movement of $^{16}O$, $^{18}O$, and N during oxynitridation.[17,21,35] We assume the energy-loss and straggling parameters to be the same as for $SiO_2$ since these oxynitride films contain at most (in the case of NO grown silicon oxynitride) $\sim 10$ at. % N.[17,21,35] This approximation may introduce a few percent error in the depth scale in the N-rich region, according to Bragg's law.[39]

## III. RESULTS AND DISCUSSION

We use $^{18}O$ labeled silicon oxide films to study silicon oxynitridation in $N^{16}O$ and $N_2^{16}O$. Figure 1 shows the depth profile of an RTO-grown $Si^{18}O_2$ film. The spectrum shows, as expected, a high $^{18}O$ concentration for the first 3 nm, followed by a fall-off to a lower value, after which the bulk silicon is reached. Somewhat surprisingly, the film also contains some $^{16}O$ near the surface, possibly from residual oxygen present as contamination on the wall of the RTP chamber. The amount of $^{16}O$ contamination should be taken into account in the following isotopic labeling experiments using $Si^{18}O_2$ starting films.

Figure 2 shows depth profiles of an $N^{16}O$-annealed (at 850 °C) $Si^{18}O_2$ film (somewhat thicker than the film in Fig.



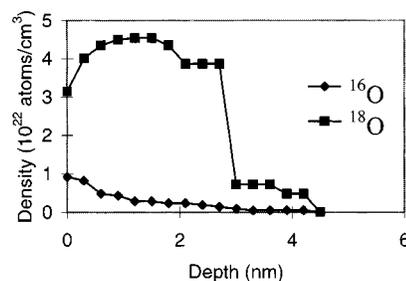FIG. 1. $^{16}O$ and $^{18}O$ depth profiles of a $\sim 3$ nm thick RTO-grown $Si^{18}O_2$ film (in 8.5 Torr $^{18}O_2$). The silicon profile is not shown. The horizontal axis is depth in nm from the surface.

1). There is little $^{16}O$ increase (compare Figs. 1 and 2) near the surface after NO annealing, and no N is observed near the surface. However, both N and $^{16}O$ are incorporated at the interface with an $N/^{16}O$ ratio of $\sim 0.7$. The gas-phase decomposition of NO is slow at the annealing temperature of 850 °C. The initial steps have a rate of $\sim 3\times 0^{-8}$ mole $L^{-1}s^{-1}$ for $NO+NO\rightarrow O_2+N_2$ and $\sim 10^{-10}$ mole $L^{-1}s^{-1}$ for $NO+NO\rightarrow N_2O+O$ at the pressure (95 Torr partial pressure) we used.[40] The fact that a similar amount of $^{16}O$ and N are distributed mainly in the region near the interface and not at the surface suggests that NO does not dissociate into N and O at the surface to a significant extent. If there was a significant amount of atomic $^{16}O$ at the surface, an oxygen-replacement reaction should have occurred there. (See the discussion for the $N_2O$ case in the next section, where atomic O is present from $N_2O$ decomposition.) The evidence implies that NO diffuses through the oxide layer most probably in molecular form and reacts near the interface. We note it has been observed previously that significant oxygen exchange occurs at the surface for $SiO_2$ films annealed in NO at 1050 °C (in addition to the nitrogen and oxygen incorporation reaction at the interface).[23] This is not in contradiction to our results as at such a high temperature, the reactions can be much more complicated because both $O_2$ and O can be present in significant amounts due to NO decomposition.[40]

Our earlier studies,[17,36] as well as work by others,[22] support the notion that NO does not remove N in the middle of the films to an appreciable degree. A possible model is that NO diffuses through the oxynitride films without interaction with the incorporated nitrogen, followed by dissociation and reaction(s) at the interface with incompletely oxidized or elemental Si. However, we cannot rule out the possibility that
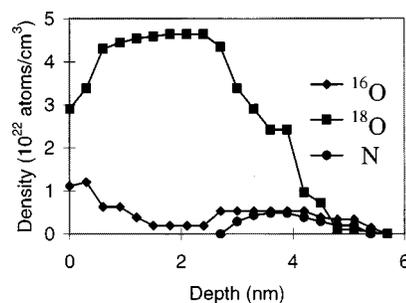


FIG. 2. $^{16}O$, $^{18}O$, and N depth profiles for a $\sim 3.8$ nm thick RTO-grown $Si^{18}O_2$ film, after NO anneal at 850 °C for 30 min.
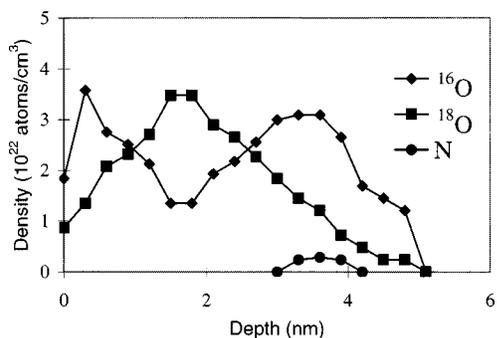
FIG. 3. Depth profiles for an $N_2O$ annealed (930 °C, 28 Torr, 60 min) $Si^{18}O_2$ film. Depth profiles for the starting ~3 nm film are shown in Fig. 1.



FIG. 4. Comparison of $^{16}O$ distributions of the oxynitride film shown in Fig. 2 after annealing in $O_2$ (6 Torr) and $N_2O$ (14 Torr), both 1 h at 930 °C. The N profile is not changed significantly.

NO can exchange nitrogen with the lattice nitrogen, without a significant change in the final nitrogen distribution. It is interesting to note that the incorporated N/O ratio of ~0.7 at the $SiO_2/Si$ interface is much higher than an oxynitride film grown in NO starting from a clean Si surface (N/O ratio ~0.1) under similar conditions.[17,18] This behavior appears to be consistent with the results of Gosset *et al.*[19] that lower NO pressure results in a higher N/O ratio. In the $SiO_2/Si$ case, NO needs to be dissolved in $SiO_2$ and thus its arrival rate at the $SiO_2/Si$ interface is very low, similar to the low NO-pressure case for the clean Si surface.

Figure 3 shows depth profiles of the two oxygen isotopes and nitrogen after annealing an ~3 nm thick $Si^{18}O_2$ film (initial depth profiles are shown in Fig. 1) in $N_2O$. Unlike the NO case, there is a significant increase in $^{16}O$, especially at the surface, accompanied by a similar amount of $^{18}O$ loss. There is also oxide growth at the interface. Finally, a small amount of nitrogen [~ 0.3 ML, where 1 ML on Si(100) $=6.8\times10^{14}$ cm$^{-2}$] is incorporated near the interface. The N concentration is much lower than in oxynitrides grown or annealed in NO (e.g., Fig. 2).

To better understand the reactions near the surface and in the middle of the film, we studied the interaction of $N_2O$ and $O_2$ with an NO-annealed $Si^{18}O_2$ film. The depth profile of the starting film is shown in Fig. 2. The initial film contains a high concentration of nitrogen at the interface, which is known[35] to suppress interfacial oxide growth in $O_2$. This makes it easier to observe what happens at the surface and in the middle of the film. As mentioned above, it is necessary to compare $N_2O$ and pure $O_2$ annealing under same conditions to see the effect attributable to $N_2O$, because $O_2$ is also present from $N_2O$ decomposition at high temperatures. Figure 4 shows a comparison of $^{16}O$ and N profiles for the relevant films. The $O_2$-annealed sample shows some $^{16}O$ increase throughout the film over that of Fig. 2, as expected. Oxide regrowth near the nitrided interface is suppressed by one order of magnitude compared to the nitrogen-free case. The $^{16}O$ incorporation at the surface is the result of an oxygen exchange, observed in earlier isotopic labeling studies.[34,41–43] The $N_2O$ results show not only more O surface incorporation than the $O_2$ case (notice the concentration falls off quickly in the first ~1.5 nm from the surface), but also a measurable amount of oxygen incorporation throughout the bulk (middle) of the film. The $^{18}O$ profiles (not
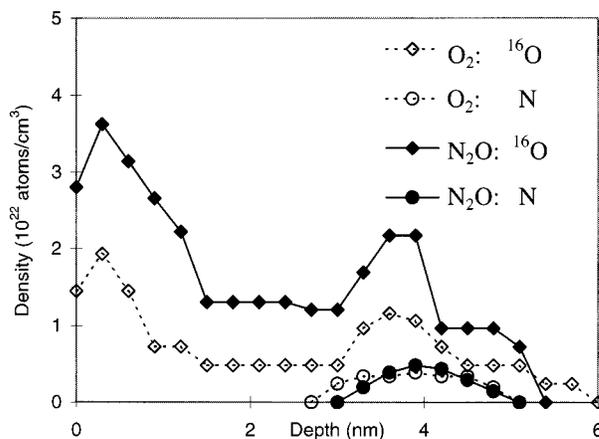
shown) are not changed near the interface, and in the rest of the film there is a total $^{18}O$ loss that roughly equals the $^{16}O$ incorporation. This suggests that oxygen from $N_2O$ can replace oxygen in $SiO_2$ or $SiO_xN_y$, most significantly at the surface but also throughout the middle of the film.

We can learn more about the oxygen replacement reaction by comparing what happens to $^{18}O$ in very thin oxide films during $N_2^{16}O$ and $^{16}O_2$ annealing. Figure 5(b) shows the profiles of a ~1.6 nm $Si^{18}O_2$ film annealed at 930 °C for 1 h in 14 Torr $N_2O$, and 6 Torr $O_2$, respectively. The pressures were chosen such that during the $N_2O$ anneal there is a similar average amount of $O_2$($O_2$ is present during the $N_2O$ anneal due to $N_2O$ decomposition), as during the $O_2$ annealing. The $N_2O$ annealed sample has a broader $^{18}O$ distribution than the $O_2$ annealed sample, though the $^{16}O$ growth near the interface is similar for both cases. This suggests that some replaced $^{18}O$ atoms near the surface, in this very thin oxide, were reincorporated near the interface during the $N_2O$ anneal.

It has been suggested based on isotopic labeling experiments that excess O atoms from $N_2O$ dissociation should be important for the oxygen replacement reaction.[31,32] An isolated oxygen atom is energetically unstable and will bond to most other atoms. In our case O atoms interact with the $SiO_xN_y/Si$ system wherever they are present (at the outer surface, the interface, or in the film). Peroxyl bridging oxygen species ($\equiv$Si–O–O–Si$\equiv$) are very probably present. They have been proposed to play an important role in oxygen exchange for pure $O_2$ oxidation,[44] and have been shown by first principle calculations[45,46] to be energetically more favorable than non-peroxyl-bridging locations. Excess oxygen atoms in other bonding configurations can also exist, but do not contribute to oxygen replacement. Both threefold coordinated oxygen[46] and fivefold coordinated Si[45,47] have been considered in first principle calculations. Because the films we use are very thin, the excess oxygen atoms may also be in a charged state by picking up electrons tunneled from the substrate. The actual mechanism of oxygen replacement may involve the formation of peroxyl bridges (Si–O–Si+O $\rightarrow$Si–O–O–Si), and then decomposition (Si–O–O–Si
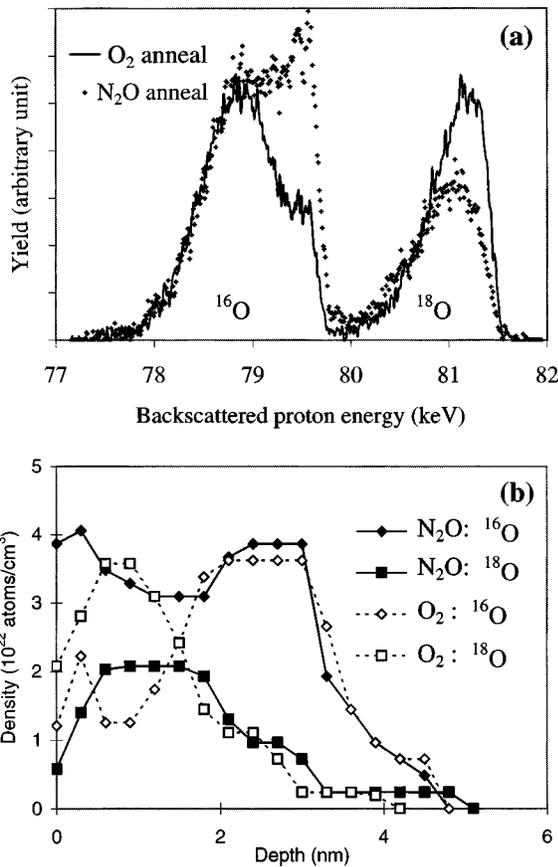
FIG. 5. Comparison of the movement of $^{18}$O after a Si$^{18}$O$_2$ film is annealed in N$_2$O (solid lines) and O$_2$ (dotted lines). Notice that the $^{18}$O distribution is wider for the N$_2$O anneal. (a) Energy spectra, (b) depth profiles.



FIG. 6. (a) Comparison of the $^{18}$O profiles after NO-annealed Si$^{16}$O$_2$ samples are again annealed in $^{18}$O$_2$ (6 Torr, 930 °C, 1 h) and $^{18}$O$_2$ (6 Torr) +N$_2$O (1.5 Torr). The addition of N$_2$O in $^{18}$O$_2$ increases the $^{18}$O incorporation at the surface significantly. (b) An ~3 nm Si$^{18}$O$_2$ sample is annealed in 6 Torr $^{18}$O$_2$ + 1.5 Torr N$_2$O at 930 °C for 1 h. There is no increase in $^{16}$O, which would have to have come from N$_2$O (cf. Fig. 1)

→Si–O–Si+O), peroxyl diffusion (Si–O–O–Si–O–Si →Si–O–Si–O–O–Si), and recombination (2 Si–O–O–Si →2 Si–O–Si+O$_2$ or Si–O–O–Si+O→Si–O–Si+O$_2$). Here O means any excess oxygen in nonperoxyl bridging positions. The reactive oxygen atoms are generated mostly in the gas phase, thus a high replacement rate is expected at the surface. MEIS detects an enhanced oxygen replacement region that extends ~1.5 nm below the surface. This may indicate that the density of excess O near the surface is larger than what is normally considered the bulk solubility of excess O in SiO$_2$. When an $^{16}$O atom recombines with an $^{18}$O atom in an already formed peroxyl bridge, it can form molecular oxygen. The molecule can then either escape from the film to account for the oxygen replacement, or diffuse further into the film and incorporate at the interface (Si$^{18}$O$_2$ and Si$^{16}$O$_2$ growth at the interface). Because oxygen replacement occurs to some extent throughout the film, peroxyl bridge formation should be possible throughout the film, not only at the surface. The relatively flat $^{16}$O distribution in the middle of the film in Fig. 4 suggests that the transport of atomic oxygen is not dominated by peroxyl diffusion.[45,46] If peroxyl diffusion is the major channel, $^{18}$O would soon dominate the diffusion species and the $^{16}$O density would quickly drop to zero with increasing depth. From the thickness of this flat region in Fig. 4, we estimate that many $^{16}$O atoms can diffuse in Si$^{18}$O$_2$ for more than ~2 nm at 930 °C without exchanging with $^{18}$O in Si$^{18}$O$_2$. This suggests channels other

than peroxyl diffusion need to be taken into account for atomic oxygen transport in SiO$_2$.

Similar processes may also be important for the enhanced silicon oxidation when O or O$_3$ is used.[48–51] Even in the case of silicon oxidation in molecular oxygen, atomic oxygen may be generated during certain stages of the oxidation reaction after the oxygen molecule dissociates at the interface. Therefore, we suggest that several observations in earlier isotopic labeling studies, namely, (1) the movement of the original oxygen distribution,[34,41] (2) the total intermixing[33] of the original oxygen distribution with the newly incorporated oxygen for very thin films (<~2 nm), as well as (3) the oxygen exchange reaction at the interface,[52] may also involve these processes.

Support for the direct involvement of O atoms, instead of molecular N$_2$O itself, in the replacement of oxygen comes from experiments with annealing both $^{16}$O-rich and $^{18}$O-rich oxynitrides in a $^{18}$O$_2$–N$_2$O mixture (Fig. 6). According to the N$_2$O gas-phase chemistry,[24–29] N$_2$O will release O atoms, which initiate a series of reactions that eventually results in the creation of N$_2$, O$_2$, and NO. We use a mixture of 6 Torr $^{18}$O$_2$ and 1.5 Torr N$_2$O so that $^{16}$O is only ~11% of all the oxygen atoms in the gas mixture. Once $^{16}$O is generated from N$_2$O dissociation, it will quickly react with $^{18}$O$_2$ through O+ O$_2$↔O$_3$, which is a more probable reaction than O+N$_2$O ↔2NO or N$_2$+O$_2$. [The reverse reaction to form N$_2$$^{18}$O, NO+NO→N$_2$O+O, is very slow in our temperature range and little N$_2$$^{18}$O could be generated. Measurements by a residual gas analyzer confirm this, showing an increase in mass 34 ($^{18}$O$^{16}$O) and no significant amount of mass 46
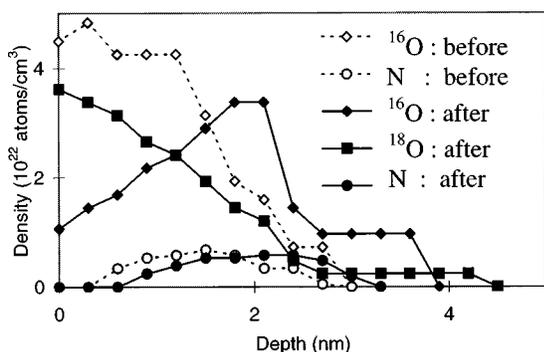
FIG. 7. NO-grown oxynitride sample before (dotted lines) and after (solid lines) 6 Torr $^{18}O_2$ + 1.5 Torr $N_2O$ anneal (900 °C, 1 h). The addition of $N_2O$ results in $^{18}O$ interaction with the film, especially near the surface. As the film grows thicker, the N distribution is also relocated towards the new interface.

($N_2$ $^{18}O$), when compared to mass 44 ($N_2$ $^{16}O$).] This shows that the $N_2O$ in the system contains predominantly $^{16}O$, and $^{16}O$ does react and readily exchange with $^{18}O_2$, which would result in the production of $^{18}O$. Therefore, $N_2O$ consists mostly of $^{16}O$. On the other hand, O, $O_2$, and $O_3$ would mostly consist of $^{18}O$. $O_3$ may participate in the reaction as a source of atomic oxygen at the surface (the size and instability of $O_3$ prohibits it from diffusing into the film). Thus, if $N_2O$ participates directly in oxygen replacement without going through the intermediate form of $O/O_3$ (e.g., a direct reaction between $N_2O$ and $SiO_2$ on the surface), the $^{16}O$ concentration would increase after annealing a $Si^{18}O_2$ film in this gas mixture. However, if $O/O_3$ is the major contribution for the oxygen replacement reaction, more $^{18}O$ would be found in an annealed $Si^{16}O_2$ sample in this gas mixture (rich in $^{18}O$) than in pure $^{18}O_2$. Figure 6(a) shows that the use of $^{18}O_2$ + $N_2O$ mixture gives a larger $^{18}O$ incorporation than the pure $^{18}O_2$ case when an ordinary oxynitride film ($Si^{16}O_xN_y$) is used. However, Fig. 6(b) shows that there is no extra $^{16}O$ incorporation at the surface using an $Si^{18}O_2$ sample, meaning $N_2O$ does not directly and appreciably replace oxygen in $SiO_2$. The $^{16}O$ concentration even decreases slightly, when compared with Fig. 1, for a $Si^{18}O_2$ starting sample. Therefore, we conclude that atomic oxygen is the major species causing the oxygen replacement.

Figure 7 shows that the nitrogen distribution of a thin oxynitride can change during $^{18}O_2$ + $N_2O$ annealing (where $^{18}O$ is present). The starting oxynitride was grown in NO on clean Si(100) to ~2 nm thickness. The film grows thicker after annealing at 900 °C in $^{18}O_2$ + $N_2O$. On the other hand, the same film shows no observable growth in pure oxygen due to the high N concentration. There is little nitrogen loss for the $^{18}O_2$ + $N_2O$ anneal, although the nitrogen distribution does move toward the new interface. When the same sample is annealed in 14 Torr $N_2O$ at 1000 °C (data not shown), in addition to a similar but larger degree of film growth and N movement, the N loss becomes appreciable (25%). Under these conditions, we are working in a regime of $N_2O$ oxynitridation with a low atomic oxygen flux that results in relatively little N removal. The movement of the N distribution toward the new interface in these cases is probably not due to

two independent reactions: N removal by O followed by N incorporation by NO (with both O and NO from $N_2O$ decomposition). The later procedure incorporates little N in the temperature and pressure range involved (e.g., see Fig. 3). It is instead quite possible that the N movement is mechanistically related to N removal by atomic oxygen.[53] It is interesting to speculate on the mechanism of the nitrogen loss. Since NO is the smallest molecule that consists of both O and N, it is plausible to assume that N leaves the film in the form of NO, analogous to $O_2$ diffusion through an $SiO_2$ film. If NO is indeed involved in N removal by atomic oxygen, it can then also diffuse further into the film, reincorporating at the new interface. In this case, a high exposure of atomic oxygen can keep most nitrogen atoms in the form of NO, until all NO molecules can diffuse to the surface and leave the film. With a low exposure of O, N removal would be less efficient and some fraction of the N should move toward the new interface by NO re-incorporation near the interface. This model may explain how nitrogen moves away from the surface and toward the new interface as the film grows thicker during low-pressure $N_2O$ annealing.

The enhanced oxidation occurs not because of the change in N distribution that in turn allows normal pure $O_2$ oxidation of $SiO_2/Si$ to proceed. There is no additional growth found during $^{18}O_2$ oxidation of a previously $N_2O$-annealed NO-grown starting oxynitride. For the thicker (>~3 nm) oxynitrided $Si^{18}O_2$ films in Fig. 4 (with N incorporated at the interface), there was very little change in the distribution of nitrogen after the $N_2O$ anneal. However, a closer look at Fig. 4 also reveals an enhanced (relative to the pure $O_2$ case) interfacial oxide growth. The location of this peak in the O distribution is at the upper part of the N distribution.

Nitrogen is argued to suppress silicon oxidation by hindering $O_2$ diffusion and/or by taking up reactive silicon sites at the interface.[35,54–56] The presence of atomic oxygen may cause oxidization of the silicon substrate when it diffuses through the oxynitride layer through mechanisms discussed above. On the other hand, when one N atom is removed by atomic oxygen to form NO, there may be several Si atoms, originally blocked, that become accessible to $O_2$ oxidation. The NO molecule can still be reincorporated back to one of these silicon atoms without leaving the film. The later mechanism can explain the enhanced oxidation at the top of the N-rich region without N loss in Fig. 4, a seemingly puzzling phenomenon.

Another contribution to the movement of the N and $^{16}O$ distributions to deeper locations in cases of $N_2O$ annealing of < 2 nm starting films (Fig. 7) may be that Si atoms outdiffuse and react with $^{18}O_2$ near the surface. Any new $Si^{18}O_2$ growth at the surface will result in previously incorporated N and $^{16}O$ atoms moving further away from the surface. This mechanism is certainly not significant with thicker starting films as in Fig. 4, where the depth of the interfacial $^{16}O/N$ distributions barely change. Si outdiffusion is also traditionally considered improbable during silicon oxidation. It has recently been shown to be absent in the oxidation of a structure of 7.6 nm $^{29}Si$ deposited on Si(111) with isotopic labeling ($^{29}Si$) techniques.[57] For the $O_2$ oxidation of a similar

starting oxynitride film as that present in Fig. 7, it was shown that $O_2$ diffuses through the oxynitride film, growing oxide underneath without oxide growth above the oxynitride film.[36] It is difficult to explain how the presence of atomic oxygen could also make Si a mobile species. It is interesting, therefore, to verify that silicon outdiffusion does not occur even with $< 2$ nm oxynitride films annealed in $N_2O$ by silicon isotopic labeling techniques.

## IV. SUMMARY

Ultrathin silicon oxide and oxynitride reactions with NO and $N_2O$ have been studied by isotopic labeling. NO is found to incorporate both O and N at the $SiO_2/Si$ interface, most probably through a mechanism in which NO diffuses through the oxide film, then dissociates and reacts with silicon at the interface. The incorporated N/O ratio is found to be rather high ($\sim 0.7$), comparable to oxynitride films grown in NO without a pre-oxide only at a much lower pressure.[19] $N_2O$ is found to cause significant O replacement, probably through its decomposition product, atomic oxygen. Atomic oxygen is also likely responsible for N removal and relocation, as well as enhanced interfacial oxide growth. In our model, both peroxyl and nonperoxyl structures are considered to explain the observed oxygen profiles and oxygen exchange. We also propose that atomic oxygen can react with incorporated N to form NO, which can explain nitrogen loss *and* nitrogen movement toward the new oxynitride/silicon interface.

## ACKNOWLEDGMENTS

[1] H. Fukuda, T. Arakawa, and S. Ohno, Jpn. J. Appl. Phys., Part 2 **29**, L2333 (1990).

[2] H. Hwang, W. Ting, B. Maiti, D. L. Kwong, and J. Lee, Appl. Phys. Lett. **57**, 1010 (1990).

[3] D. Wristers, L. K. Han, T. Chen, H. H. Wang, D. L. Kwong, M. Allen, and J. Fulford, Appl. Phys. Lett. **68**, 2094 (1996).

[4] D. Mathiot, A. Straboni, E. Andre, and P. Debenest, J. Appl. Phys. **73**, 8215 (1993).

[5] E. C. Carr and R. A. Buhrman, Appl. Phys. Lett. **63**, 54 (1993).

[6] K. S. Krisch, M. L. Green, F. H. Baumann, D. Brasen, L. C. Feldman, and L. Manchanda, IEEE Trans. Electron Devices **43**, 982 (1996).

[7] M. Bhat, L. K. Han, D. Wristers, J. Yan, and D. L. Kwong, Appl. Phys. Lett. **66**, 1225 (1995).

[8] G. Rangelov, J. Stober, B. Eisenhut, and T. Fauster, Phys. Rev. B **44**, 1954 (1991).

[9] B. Röttger, R. Kliese, and H. Neddermeyer, J. Vac. Sci. Technol. B **14**, 1051 (1996).

[10] M. D. Wiggins, R. J. Baird, and P. Wynblatt, J. Vac. Sci. Technol. **18**, 965 (1981).

[11] M. Nishijima, H. Kobayashi, K. Edamoto, and M. Onchi, Surf. Sci. **137**, 473 (1984).

[12] H. Kato, K. Sawabe, and Y. Matsumoto, Surf. Sci. **351**, 43 (1996).

[13] T. Kubo, T. Ema, A. Atli, T. Aruga, N. Takagi, and M. Nishijima, Surf. Sci. **382**, 214 (1997).

[14] E. G. Keim and A. van Silfhout, Surf. Sci. **216**, L337 (1989).

[15] J. Stober, B. Eisenhut, G. Rangelov, and T. Fauster, Surf. Sci. **321**, 111 (1994).

[16] Y. Taguchi, M. Fujisawa, Y. Kuwahara, and M. Onchi, Surf. Sci. **217**, L413 (1989).

[17] E. P. Gusev, H. C. Lu, T. Gustafsson, E. Garfunkel, M. L. Green, and D. Brasen, J. Appl. Phys. **82**, 896 (1997).

[18] J. A. Aboaf, J. Electrochem. Soc. **118**, 1370 (1971).

[19] L. G. Gosset, J.-J. Ganem, I. Trimaille, S. Rigo, F. Rochet, G. Dufour, F. Jolly, F. C. Stedile, and I. J. R. Buaumvol, Nucl. Instrum. Methods (to be published).

[20] R. Hedge, B. Maiti, and P. Tobin, J. Electrochem. Soc. **144**, 1081 (1997).

[21] H. C. Lu, E. P. Gusev, T. Gustafsson, E. Garfunkel, M. L. Green, D. Brasen, and L. C. Feldman, Appl. Phys. Lett. **69**, 2713 (1996).

[22] Z.-Q. Yao, J. Appl. Phys. **78**, 2906 (1995).

[23] I. J. R. Baumvol, J.-J. Ganem, L. G. Gosset, I. Trimaille, and S. Rigo, Appl. Phys. Lett. **72**, 2999 (1998).

[24] P. J. Tobin, Y. Okada, S. A. Ajuria, V. Lakhotia, W. A. Feil, and R. I. Hedge, J. Appl. Phys. **75**, 1811 (1994).

[25] K. A. Ellis and R. A. GBuhrman, Appl. Phys. Lett. **68**, 1696 (1996).

[26] D. L. Baulch, D. D. Drysdale, and D. G. Horne, *Evaluated Kinetic Data for High Temperature Reactions* (Butterworths, London, 1973), Vol. 2.

[27] H. Loirat, F. Caralp, W. Forst, and C. Schoenenberger, J. Phys. Chem. **89**, 4586 (1985).

[28] W. Forest, J. Phys. Chem. **86**, 1776 ()1982.

[29] A. Gupta, S. Toby, E. P. Gusev, H. C. Lu, Y. Li, M. L. Green, T. Gustafsson, and E. Garfunkel, Prog. Surf. Sci. **59**, 103 (1998).

[30] K. Kim, Y. H. Lee, M.-S. Suh, C.-J. Youn, K.-B. Lee, and H. J. Lee, J. Electrochem. Soc. **143**, 3372 (1996).

[31] J.-J. Ganem, S. Rigo, I. Trimaille, I. J. R. Baumvol, and F. C. Stedile, Appl. Phys. Lett. **68**, 2366 (1996).

[32] I. J. R. Bauymvol, F. C. Stedile, J.-J. Ganem, I. Trimaille, and S. Rigo, Appl. Phys. Lett. **70**, 2007 (1997).

[33] E. P. Gusev, H. C. Lu, T. Gustafsson, and E. Garfunkel, Phys. Rev. B **52**, 1759 (1995).

[34] H. C. Lu, T. Gustafsson, E. P. Gusev, and E. Garfunkel, Appl. Phys. Lett. **67**, 1742 (1995).

[35] H. C. Lu, E. P. Gusev, T. Gustafsson, and E. Garfunkel, J. Appl. Phys. **81**, 6992 (1997).

[36] E. P. Gusev, H. C. Lu, E. Garfunkel, T. Gustafsson, D. Brasen, M. L. Green, and W. M. Lennard, J. Appl. Phys. **84**, 2980 (1998).

[37] J. F. van der Veen, Surf. Sci. Rep. **5**, 199 (1985).

[38] R. M. Tromp, M. Copel, M. C. Reuter, M. H. von Hoegen, J. Speidell, and R. Koudijs, Rev. Sci. Instrum. **62**, 2679 (1991).

[39] L. C. Feldman and J. W. Mayer, *Fundamentals of Surface and Thin Film Analysis* (Prentice Hall, Englewood Cliffs, NJ, 1986).

[40] W. G. Mallard, F. Westley, J. T. Herron, and R. F. Hampton, NIST Chemical Kinetics Database, NIST Standard Reference Data, Gaithersburg, MD, 1994.

[41] C. J. Han and C. R. Helms, J. Electrochem. Soc. **135**, 1824 (1988).

[42] F. Rochet, S. Rigo, M. Froment, C. d'Anterroches, C. Maillot, H. Roulet, and G. Dufour, Adv. Phys. **35**, 237 (1986).

[43] J.-J. Ganem, G. Battistig, S. Rigo, and I. Trimaille, Appl. Surf. Sci. **65/66**, 647 (1993).

[44] J.-J. Ganem, I. Trimaille, P. André, S. F. Rigo, F. C. Stedile, and I. J. R. Baumvol, J. Appl. Phys. **81**, 8109 (1997).

[45] D. R. Hamann, Phys. Rev. Lett. **81**, 3447 (1998).

[46] K.-O. Ng, Ph.D. thesis, Rutgers University, 1999.

[47] A. Pasquarello, M. S. Hybertsen, and R. Carr, Nature (London) **396**, 58 (1998).

[48] T. Engel, Surf. Sci. Rep. **18**, 91 (1993).

[49] J. R. Engstrom, D. J. Bonser, M. M. Nelson, and T. Engel, Surf. Sci. **256**, 317 (1991).

[50] J. R. Engstrom, D. J. Bonser, and T. Engel, Surf. Sci. **268**, 238 (1992).

[51] A. Kazor, R. Gwilliam, and I. W. Boyd, Appl. Phys. Lett. **65**, 412 (1994).

[52] T. Åkermark, L. G. Gosset, J.-J. Ganem, I. Trimaille, I. Vickridge, and S. Rigo (unpublished).

[53] E. C. Carr, K. A. Ellis, and R. A. Buhrman, Appl. Phys. Lett. **66**, 1492 (1995).

[54] E. P. Gusev, H. C. Lu, E. Garfunkel, T. Gustafsson, and M. L. Green, IBM J. Res. Dev. **43**, 265 (1999).

[55] M. L. Green, D. Brasen, L. C. Feldman, W. Lennard, and H. T. Tang, Appl. Phys. Lett. **67**, 1600 (1995).

[56] S. Dimitrijev, D. Sweatman, and H. B. Harrison, Appl. Phys. Lett. **62**, 1539 (1993).

[57] I. J. R. Baumvol, C. Krug, F. C. Stedile, F. Gorris, and W. H. Schulte, Phys. Rev. B **60**, 1492 (1999).